

Original Article

miR-146b expression is upregulated in the lung of pulmonary fibrosis mice

Jing Chai^{1,2}, Zhihong Li³, Bin Zhou¹, Honglin Zhu¹, Xiaoyun Xie⁴, Xiaoxia Zuo¹

¹Department of Rheumatology, Xiangya Hospital, Central South University, Changsha, Hunan, China; ²Department of Rheumatology, Peking University Third Hospital, Beijing, China; ³Division of General Surgery, Shanghai Pudong New District Zhoupu Hospital, Shanghai, China; ⁴Division of Geriatrics, Tongji Hospital, School of Medicine, Tongji University, Shanghai, China

Received October 31, 2015; Accepted December 26, 2015; Epub February 1, 2016; Published February 15, 2016

Abstract: Objective: This study aimed to investigate the expressions of miR-146b and miR-503 in the lung of pulmonary fibrosis (PF) mice and their influence on the PF. Methods: Female C57BL/6 mice aged 7 weeks were randomized into control group (n=10) and PF group (n=20). PF was induced by intratracheal administration of bleomycin. The lung was collected for hematoxylin-eosin staining, Masson's trichrome staining and detection of genes related to PF. RT-PCR was employed to detect the miR-146b expression. Bioinformatics was used to predict the target genes of miR-146b. RT-PCR and Western blot assay were conducted to validate the expressions of these target genes in the lung of PF mice. Results: miR-146b expression increased significantly in the lung of PF mice as compared to control group (P<0.01). Target genes of miR-146b included irak, siah2, klf4, mmp16, notch1 and foxO3. In PF mice, the expressions of foxO3 and siah2 reduced markedly and were negatively related to the miR-146b expression. Conclusion: In mice with bleomycin induced PF, miR-146b expression increases significantly in the lung and may exert its biological effects via targeting foxO3 and siah2.

Keywords: Systemic sclerosis, pulmonary fibrosis, miR-146b, foxO3

Introduction

Systemic sclerosis (SSc) is a connective tissue disease of unknown causes and characterized by multiple-organ fibrosis secondary to vascular and immune dysfunction as well as excess proliferation of fibroblasts. Pulmonary fibrosis (PF) is one of major causes of death in SSc patients. PF is characterized by alveolar epithelial injury, infiltration of inflammatory cells, excess proliferation of fibroblasts and deposition of excess collagens in the pulmonary interstitium. Currently, there are no specific drugs used for the therapy of PF and thus PF has a poor prognosis. miRNA may regulate almost all the cellular processes. Available studies have shown that several miRNAs including miR-21, miR-29, miR-145, miR-31 and miR-26a are closely related to the PF. miR-21 expression increases significantly in the lung of mice with bleomycin induced PF and PF patients. miR-21 can act on smad7 to attenuate the negative regulation of TGF- β signaling pathway, an

important pathway involved in the pathogenesis of PF [1]. However, miR-29 expression reduces in the PF. In fibroblasts with miR-29 knock-out, the expressions of genes related to collagen generation and extracellular matrix (ECM; such as laminin and integrins) remodeling increased. In addition, miR-29 is also regulated by the TGF- β signaling pathway [2]. miR-145 is involved in the differentiation of myofibroblasts and can act on KLF4 to promote the expression of α -SMA, a myofibroblast specific protein. In the lung of PF patients, miR-145 expression increases, while miR-145^{-/-} mice are resistant to bleomycin induced PF [3]. miR-31 is a miRNA which can inhibit PF. miR-31 may directly act on integrin α and RhoA to inhibit the activation of fibroblasts [4]. miR-26a expression reduces in PF, and CTGF is a target gene of miR-26a. The down-regulated miR-26a expression significantly increases CTGF protein expression, which leads to the excess production of collagens, resulting in PF [5]. Our previous study showed 6 differentially expressed miRNAs in the fibrotic

miR-146b upregulated in pulmonary fibrosis

Table 1. Expressions of miRNAs in the fibrotic skin and fibrotic lung

miRNA	Skin	Lung	Target gene
miR-21 [16]	↑	↑	Smad7
miR-31 [17]	↑	↓	Integrin α rhoA
miR-145 [18]	↓	↑	KLF4
miR-29b [19]	↓	↓	LN, integrin et al
miR-503	↑		-
miR-146b	↑		-

skins of scleroderma patients: miR-21, miR-31, miR-146b, miR-503, miR-145 and miR-29b [6]. However, the expressions of these miRNAs are different from those in PF (**Table 1**). miR-146b expression has never been studied in PF. This study aimed to investigate the miR-146b expression and its significance in PF, which may help to understand the role of regulatory network of miRNAs in SSc.

Materials and methods

Materials

Specific pathogen-free (SPF) female C57BL/6 mice (n=30) aged 7 weeks and weighing 48-22 g were purchased from the SLAC Animal Center (Hunan). Following reagents were used in the present study: bleomycin hydrochloride injection (Nippon Kayaku Co., Ltd.), Masson solution and hematoxylin-eosin (H-E) staining solution (Nanjing Jiancheng Biotechnology Institute), microRNA reverse transcription kit (Qiagen Sample & Assay Technologies, USA), microRNA SYBR Premix Ex Taq (Qiagen Sample & Assay Technologies, USA), RNA reverse transcription kit (TAKARA, Japan), SYBR Premix Ex Taq (TAKARA, Japan), DNA Marker (Sigma, USA), TEMED (Sigma, USA), RIPA lysis buffer and PMSF (Beijing Beyotime Biotechnology Institute), rabbit anti-GAPDH, irak, siah2, klf4, mmp16, notch1 and foxO3 antibodies (CST, USA), goat anti-rabbit IgG (Wuhan Boster Biotechnology Co., Ltd), thermal cycler (Swift MaxPro; Perkin-Elmer, USA), fluorescence thermal cycler (Applied Biosystems 7500; ABI, USA).

Methods

Animals were randomly assigned into control group (n=10) and PF group (n=20). After anesthesia, a middle incision was made at the neck and the muscles were separated to expose the trachea. Then, 100 μ l of normal saline (control

group) or bleomycin solution (3.5 mg/kg; PF group) was administered into the trachea. The mouse was rapidly rotated for 1 min to allow the normal saline or bleomycin solution to be evenly distributed in the lung. After wound closure, animals were placed back to cages. Body weight was monitored once weekly. The lung was collected under an aseptic condition and processed for HE staining, Masson's trichrome staining and detection of mRNA expressions of genes related to PF (COL1A1, COL1A2, Fn and α -SMA), aiming to validate whether the animal model was successfully established.

HE staining: The lung was cut into 2-3 mm blocks, embedded in paraffin and sectioned. Lung sections were subjected to sequential treatment with xylene, ethanol, ethanol, 80% ethanol, 70% ethanol, and double-distilled water for deparaffinization. After hydration and counterstaining with hematoxylin, sections were dehydrated and mounted, and observed under a light microscope.

Masson's trichrome staining: After deparaffinization and hydration, sections were subjected to Masson's trichrome staining. In brief, sections were treated with a solution containing hematoxylin and ferric oxide for 10 min after hydration. After treatment with ethanol-hydrochloride treatment, washing with double-distilled water, treatment with ammonia solution, washing with double-distilled water for 1 min, and Acid Fuchsin staining for 10 min, sections were treated with acetic acid solution for 1 min, phosphomolybdic acid solution for 2 min, acetic acid solution for 1 min and then aniline blue for 2 min. Following treatment with acetic acid solution for 1 min, 95% ethanol for 5 min and 100% ethanol for 5 min, sections were incubated with xylene for 5 min thrice and finally mounted with neutral gum.

Real-time fluorescence PCR: Total RNA was extracted with Trizol reagent and subjected to agarose gel electrophoresis to examine the integrity and purity of total RNA. RNA concentration was determined by ultraviolet spectrophotometry (Q3000 spectrophotometer). In brief, 2 μ l of total RNA was collected, and the A260 and A280 were determined at 260 nm and 280 nm, respectively. The A260/A280 was calculated. RNA with A260/A280 at 1.8-2.0 was used in following experiments. Then, 1 μ g of total RNA was used in PCR. Mixture (20 μ l) for reverse transcription was prepared accord-

miR-146b upregulated in pulmonary fibrosis

Table 2. Primers used in the present study

Genes	Primers
miR-146b	5'-UGAGAACUGAAUCCAAGGCU-3'
GAPDH	Forward: 5'-TGTCTCCGTCGTGGATGCA-3' Reverse: 5'-TTGCAGTTGAAGTCGCAGGAG-3'
COL1A1	Forward: 5'-GACATGTTTCAGCTTTGTGGACCTC-3', Reverse: 5'-GGGACCCTTAGCCATTGTGTA-3'
COL1A12	Forward: 5'-TGCTTGCAGTAACTTCGTGCCTA-3', Reverse: 5'-CATGGGACCATCAACACCATC-3'
Fibronectin	Forward: 5'-GCTTTGGCAGTGGTCATTTTCAG-3' Reverse: 5'-ATTCCCGAGGCATGTGCAG-3'
α-SMA	Forward: 5'-AAGAGCATCCGACACTGCTGAC-3' Reverse: 5'-AGCACAGCCTGAATAGCCACATAC-3'
KLF4	Forward: 5'-GCCCAACACACAGACTTC-3' Reverse: 5'-GGCAGGAAAGGAGGGTAGTT-3'
MMP16	Forward: 5'-TGGAAGAAGGTTGGATTTTCG-3' Reverse: 5'-GTCAGTCGGTGAAGGTAGC-3'
NOTCH1	Forward: 5'-AACAGTGCCGAATGTGAGTG-3' Reverse: 5'-CGCAGAAAGTGAAGGAGTT-3'
FOXO3	Forward: 5'-TACCGTGTGGACCTTCGT-3' Reverse: 5'-TACCGTGTGGACCTTCGT-3'
IRAK1	Forward: 5'-TACCGTGTGGACCTTCGT-3' Reverse: 5'-TACCGTGTGGACCTTCGT-3'
SIAH2	Forward: 5'-CTGTGGACTGGGTGATGATG-3' Reverse: 5'-CCAATGAGGAGGACGATGG-3'

ing to the manufacturer's instructions. This mixture was incubated at 37°C for 60 and then 95°C for 5 min. SYBR Green was used to label DNA (QIAGEN miScript SYBR Green PCR). Primers for miR-146b were synthesized in QIAGEN (Table 2). Applied Biosystems 7500 Real-time PCR System was employed for RT-PCR. Conditions for RT-PCR were as follows: 95°C for 15 min, 40 cycles of 94°C for 15 s (denaturation), 55°C for 30 s (annealing) and 70°C for 30 s (extension). The melting curve was obtained, and Ct value determined. Data were analyzed with 2^{-ΔΔCT} method.

Detection of protein expression by Western blot assay: Tissues were collected and lysed in RIPA lysis buffer (1 mg of tissues per 10 μl of RIPA buffer) and protease inhibitor PMSF (1:100). After centrifugation, protein concentration was determined via ultraviolet spectrophotometry. Then, 20 μg of proteins per sample were loaded and separated by SDS-PAGE and then transferred onto PVDF membrane. The membrane was incubated in 5% non-fat milk and then treated with primary antibody at 4°C over night according to manufacturer's instructions. After incubation with HRP conjugated secondary antibody (1:3000), the membrane was washed

and subsequently treated with ECL chemiluminescence solution for 3 min. After exposure to a film, the protein bands were scanned into a computer and analyzed with Quantity One.

Bioinformatics and morphological examination: The prediction and screening of target genes were conducted with online databases Targetscan (www.targetscan.org), miRanda (<http://www.microrna.org/microrna/home.do>), PicTar (<http://pic-tar.mdc-berlin.de/>) and PubMed. PF was evaluated after Masson's trichrome staining with Image-Pro Plus 6.0. In brief, 5 fields were randomly selected from each section rich in collagens (200×), and the proportion of positive area was determined, followed by averaging.

Statistical analysis

Statistical analysis was performed with SPSS version 18.0 and data are expressed as mean ± standard deviation (X ± S). F test was employed for the examination of normal distribution of quantitative data, and t test for the comparisons of data with normal distribution between two groups. Wilcoxon rank sum test was used for comparisons of data with abnormal distribution. A value of P<0.05 was considered statistically significant.

Results

Lung morphology of PF mice

In control group, HE staining and Masson's trichrome staining showed the lung structure was clear, alveolar terminal bronchioles, alveolar ducts and alveolar sacs were regularly arranged, there was no interstitial thickening, no infiltration of inflammatory cells and no deposition of collagens. In PF group, HE staining showed the lung structure was disordered, tissue consolidation was found in a fraction of lung tissues, and some normal alveoli were replaced with merged, cystic cavities where were surrounded by thickened fibrous tissues. Masson's trichrome staining revealed a large amount of blue collagens in the lung interstitium, (P<0.05) (Figures 1 and 2).

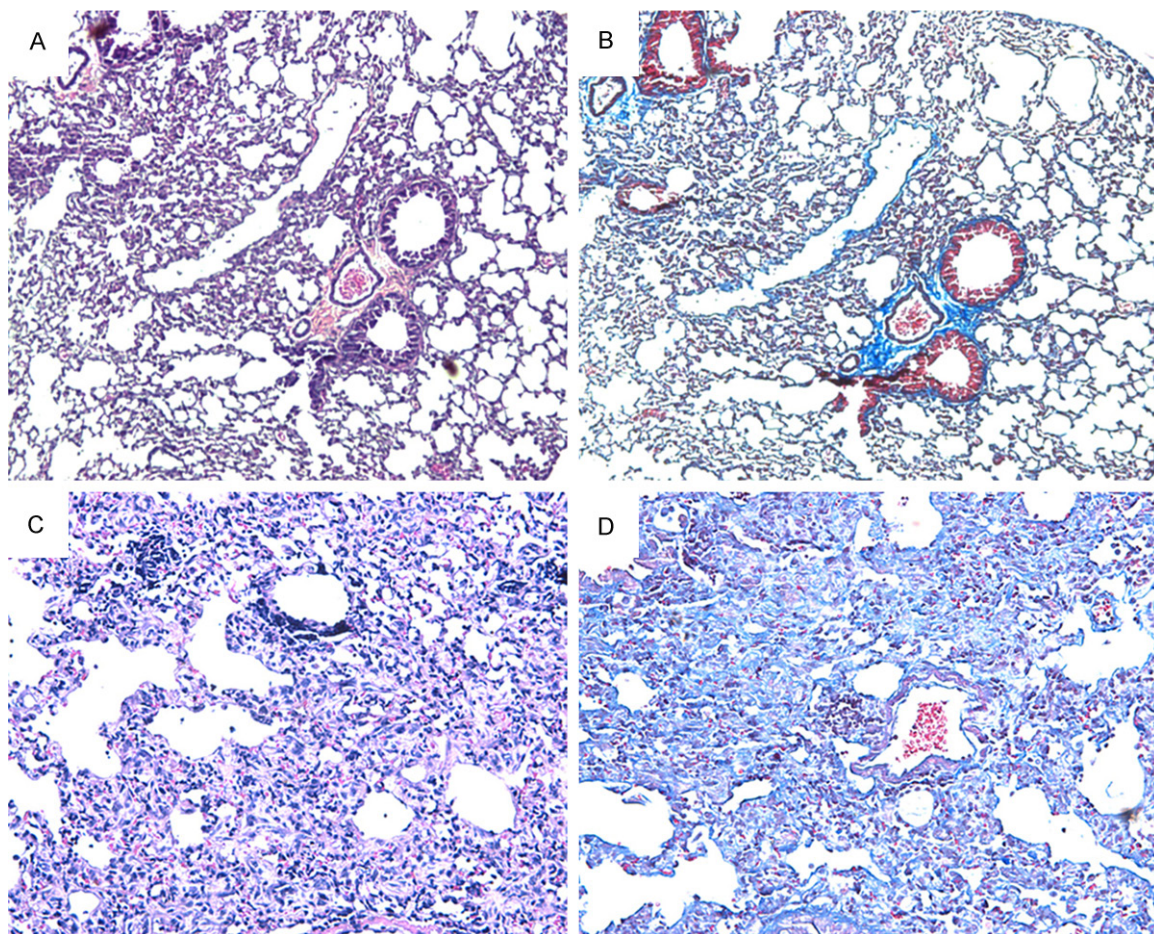


Figure 1. HE staining and Masson's trichrome staining of the lung in both groups. A: HE staining of control group ($\times 200$); B: Masson's trichrome staining of control group ($\times 200$); C: HE staining of PF group ($\times 200$); D: Masson's trichrome staining of PF group ($\times 200$).

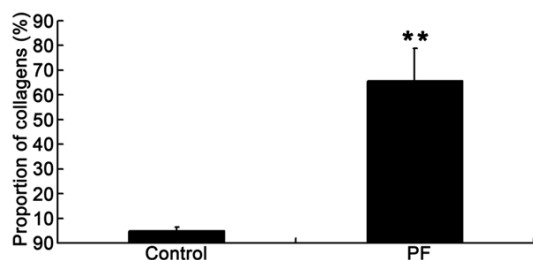


Figure 2. Collagen content in the lung of mice in both groups. Note: Proportion of collagens in the lung (** $P < 0.01$ vs control group).

Up-regulated expressions of proteins related to fibrosis

Above findings confirmed that the bleomycin induced PF was successfully established in mice by macroscopical and histological examination. Then, the expressions of genes related to fibrosis (COL1A1, COL1A2, Fibronectin and

α -SMA) were detected in the lung. Results showed the mRNA expressions COL1A1, COL1A2, fibronectin and α -SMA increased dramatically in the lung of PF mice as compared to mice in control group ($P < 0.05$) (Figure 3).

Up-regulated miR-146b expression in the lung of PF mice

Real time PCR showed the miR-146b expression in the lung of PF mice was significantly higher than in control mice ($P < 0.01$) (Figure 4).

Target genes of miR-146b

In the present study, the target genes of miR-146b were predicted with Targetscan (www.targetscan.org) and miRanda (<http://www.microrna.org/>), and PicTar (<http://pictar.mdc-berlin.de/>), and nucleotide database of NCBI (<http://www.ncbi.nlm.nih.gov/>) and relevant literatures in the PubMed were searched. Finally,

miR-146b upregulated in pulmonary fibrosis

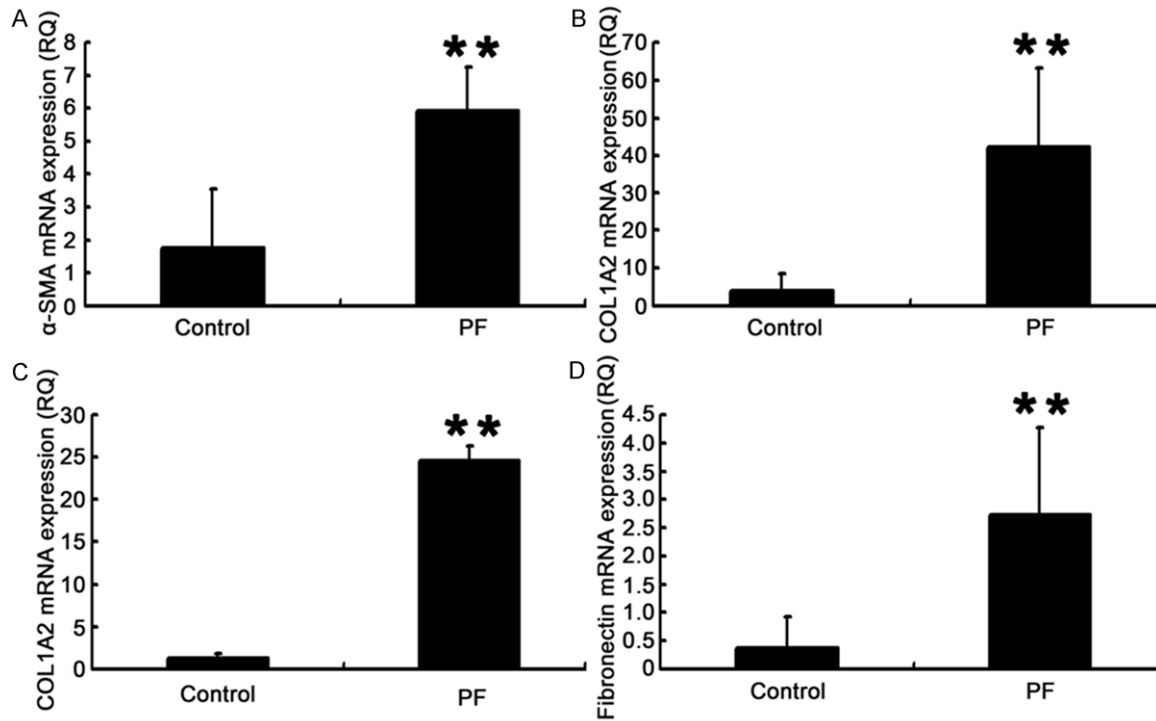


Figure 3. mRNA expressions of genes related to fibrosis in the lung (real time PCR). A: α-SMA; B: Fn; C: COL1A1; D: COL1A2. (**P<0.01).

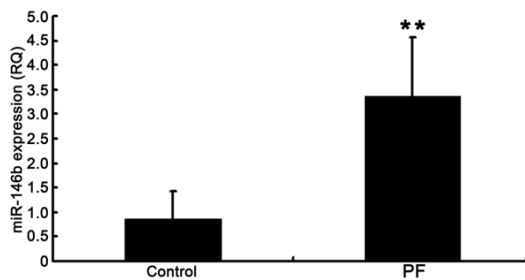


Figure 4. miR-146b expression in the lung of mice (real time PCR). **P<0.01 vs control group.

6 genes related to fibrosis were identified: *irak*, *siah2*, *klf4*, *mmp16*, *notch1* and *foxO3* (Figure 5).

Down-regulated foxO3 expression in the lung of PF mice

We further detected the mRNA expressions of predicted target genes of miR-146b. Our results showed significant differences in the mRNA expressions of *foxO3*, *siah2* and *mmp16* between two groups (Figure 6) (P<0.05). In PF group, the mRNA expressions of *foxO3* and *siah2* reduced markedly and were negatively related to miR-146b expression, but *mmp16*

expression increased dramatically in PF group. Significant difference was not found in the mRNA expressions of other target genes of miR-146b (Figure 7).

miRNA may inhibit the translation of target genes, only leading to the reduced protein expression of target genes. Thus, the protein expressions of *mmp16* and *foxO3* were also detected in the lung. Results showed the *mmp16* protein expression was comparable between two groups (Figure 8), but *foxO3* protein expression reduced markedly in PF group (P<0.05 vs control group) (Figure 9).

Discussion

Bleomycin induced PF is characterized by alveolitis at early stage, which then progresses into chronic fibrosis without treatment. Bleomycin induced PF may effectively mimic the progression of interstitial lung diseases in human and thus often used to investigate molecular signaling pathways involved in the pathogenesis of PF. Mice may develop body weight loss at 1 week after bleomycin induced PF and thereafter, body weight increases and restores to normal. In the present study, the

miR-146b upregulated in pulmonary fibrosis

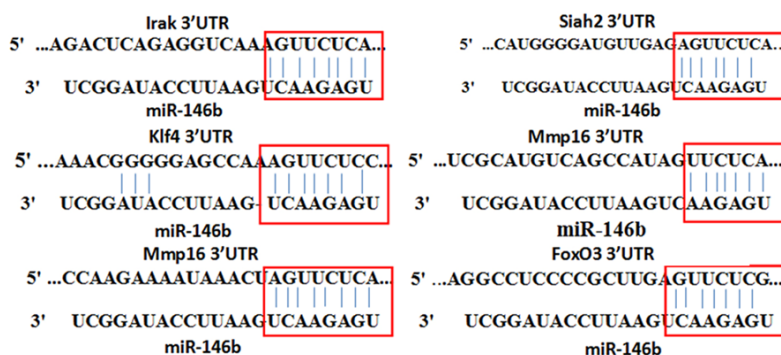


Figure 5. Potential binding sites of miR-146b to predicted target genes (target scan).

body weight in PF mice reduced significantly when compared with control group. HE staining showed the lung structure was disordered, some alveoli merged, and a fraction of lung tissues consolidated. Masson's trichrome staining showed a large amount of blue collagens which corresponded to the red collagens in HE staining. Moreover, we also detected the mRNA expressions of fibrosis related genes in the lung. Results showed the mRNA expressions of α -SMA, Fn, COL1A1 and COL1A2 increased significantly in mice after intratracheal administration of bleomycin. These findings suggest that PF animal model was successfully established.

In the fibrotic skins, the expressions of miR-21, miR-31, miR-146b and miR-503 increase significantly, but those of miR-145 and miR-29b are down-regulated. There is evidence showing that the expressions of miR-31 and miR-145 in the PF show different tendency from those in the fibrotic skins. Our results showed miR-146b expression increased significantly in the PF, as observed in the fibrotic skins. miR-146b has been found to be related to inflammation: the presence of inflammation is usually accompanied by the increase in miR-146b expression, and pro-inflammatory cytokines may up-regulate the miR-146b expression [7-10]. It has been proposed the miR-146b may inhibit the interleukin-1 receptor-associated kinase (IRAK1) and TNF receptor-associated factor (TRAF6) to negatively regulate inflammation [7]. In recent years, studies reveal that miR-146b plays an important role in the myocardial fibrosis and phenotypic conversion of fibroblasts [11, 12]. In the present study, results showed miR-146b expression increased significantly in PF mice, and remained at a high level. Generally,

the lung injury in PF within 1-7 days is characterized by alveolitis, and chronic fibrosis is present at 14 d. Thus, the sustained increase in miR-146b expression may not completely explained by the inflammation alone. We speculate that the increased miR-146b plays a crucial role in the transformation from inflammation into fibrosis. Fibroblasts express miR-146b, which is regulated by TGF- β . In addition,

miR-146b may also act on ubiquitin related protein UBE2D2 and matrix metalloproteinases MMP16 to inhibit the degradation of ECM [11, 13]. In our study, bioinformatics was employed to predict target genes of miR-146b and a total of 6 genes were identified. Of them, the mRNA expressions of foxO3 and siah2 reduced, but mmp16 mRNA expression increased, and significant difference was not observed in other genes. Further validation with Western blot assay revealed that mmp16 protein expression remained unchanged. Thus, the role of mmp16 as a target gene of miR-146b could be excluded. siah2 is an E3 ubiquitin ligase and siah2 activation may promote the degradation of smad7 in the TGF- β signaling pathway [14], leading to the inhibition of fibrosis because smad7 is able to negatively regulate the profibrotic activity of TGF- β . Forkhead box protein foxO3 is a transcriptional activator related to apoptosis. In idiopathic pulmonary fibrosis, the FOXO3 activity reduces in the fibroblasts [15]. Low FOXO3 activity may down-regulate CAV-1 to inhibit Fas expression, reducing the collagen-mediated apoptosis of fibroblasts. In our study, the FOXO3 expression reduced significantly in the lung of PF mice and was negatively related to miR-146b expression. Thus, we speculate that pro-inflammatory cytokines in the stage of inflammation up-regulate the miR-146b expression in fibroblasts, which inhibits the FOXO3 transcription and then decrease Fas expression, leading to the inhibition of fibroblasts. However, in late stage (stage of fibrosis), TGF- β may stimulate the sustained expression of miR-146b, which further increases fibroblasts, forming a positive feedback and resulting in PF. Of note, we can not deny the negative regulation of miR-146b on inflammation and fibrosis.

miR-146b upregulated in pulmonary fibrosis

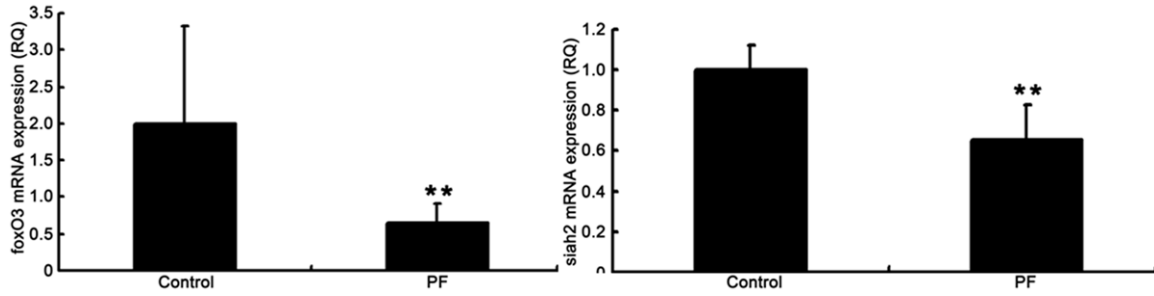


Figure 6. mRNA expressions of foxO3 and siah2 in the lung. **P<0.01 vs control group.

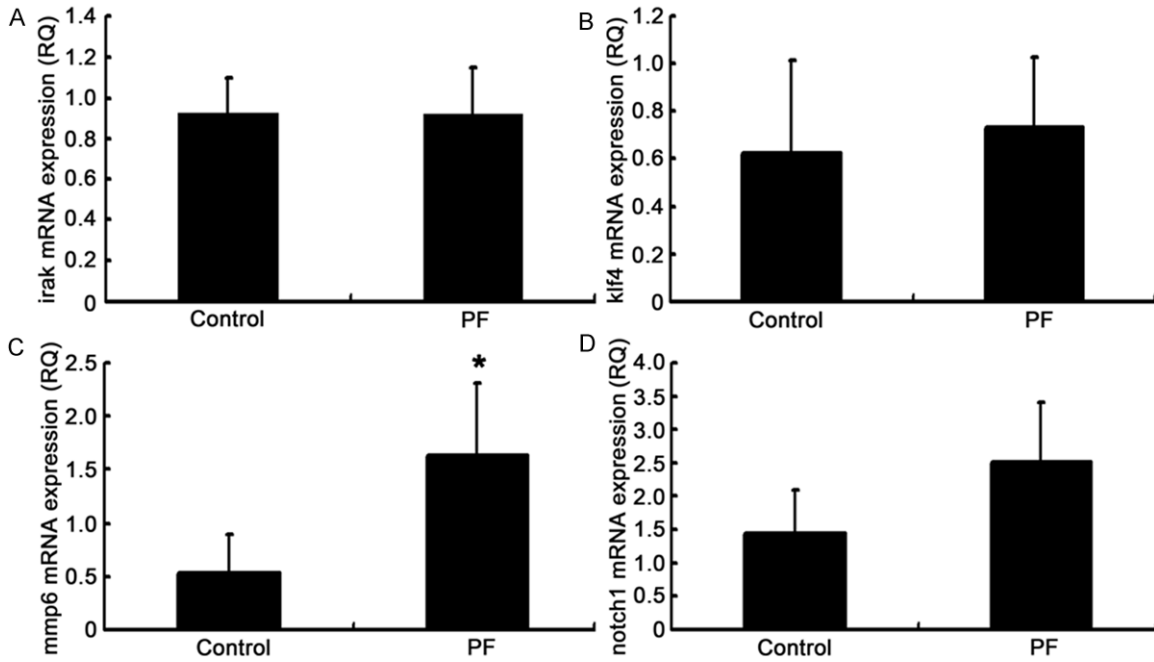


Figure 7. mRNA expressions of irak, notch1, mmp16 and kif4 in the lung. *P<0.05 vs control group.

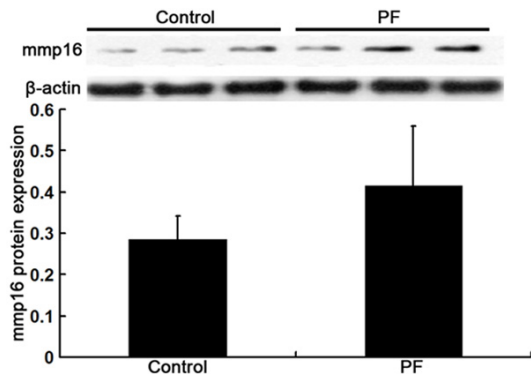


Figure 8. mmp16 protein expression (Western blot assay).

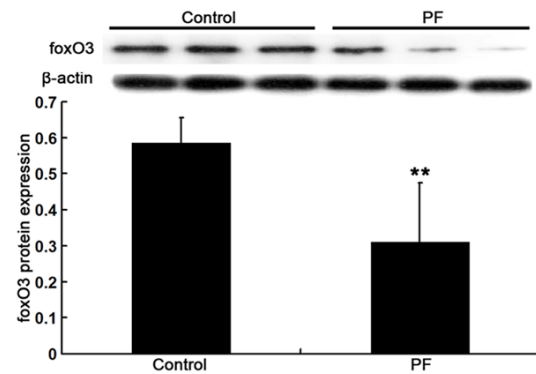


Figure 9. foxO3 protein expression in the lung (Western blot assay). **P<0.01 vs control group.

miR-146b may act on SIAH2 to up-regulate smad7 expression and inhibit the TGF- β -induced production of ECM, which also sup-

presses the ECM induced apoptosis of fibroblasts. Several studies have confirmed that miR-146b may act on IRAK1 to inhibit

inflammation. However, in the present study, the mRNA expression of *orak1* remained unchanged in the lung of PF mice. It is possible that miR-146b is mainly expressed in the fibroblasts during the stage of fibrosis and the target genes of miR-146b are cell-specific.

Although miRNAs have the potential in the therapy of diseases, it has a long way to go before anti-fibrotic therapy is conducted targeting miR-146b. In the inflammation related to interstitial lung diseases, which inflammation related signaling pathway is mainly regulated by miR-146 and the clinical significance of this pathway are largely unclear. In addition, whether increased miR-146 expression in the inflammation may further induce fibrosis and whether inhibition of miR-146 expression may deteriorate inflammation are still needed to be elucidated. There is evidence showing that the miRNA expressing profile is different between fibrotic tissues, which might be helpful for the prediction of fibrosis in different tissues. Currently, most studies on miR-146 are observational, and more studies are required before the application of miR-146 as a target in the therapy of PF.

Conclusion

In bleomycin induced PF, miR-146b expression increases significantly, but *foxO3* expression reduces dramatically in the lung, and bioinformatics analysis shows *foxO3* is a target gene of miR-146b. Thus, miR-146b may inhibit *foxO3* expression to facilitate PF.

Acknowledgements

This work supported by National Natural Science Foundation of China (Grant No. 81200244 and No. 81570738) to Xiaoyun Xie, National Natural Science Foundation of China (81373206, 81401357) to Xiaoxia Zuo, Fundamental Research Funds for the Central South University; and supported by Seed Foundation of Peking University Third Hospital.

Disclosure of conflict of interest

None.

Address correspondence to: Dr. Xiaoxia Zuo, Department of Rheumatology, Xiangya Hospital, Central South University, 87 XiangYa Road,

Changsha 41000, Hunan, China. E-mail: susanzuo@hotmail.com

References

- [1] Nakasa T, Miyaki S, Okubo A, Hashimoto M, Nishida K, Ochi M and Asahara H. Expression of microRNA-146 in rheumatoid arthritis synovial tissue. *Arthritis Rheum* 2008; 58: 1284-1292.
- [2] Yamasaki K, Nakasa T, Miyaki S, Ishikawa M, Deie M, Adachi N, Yasunaga Y, Asahara H and Ochi M. Expression of MicroRNA-146a in osteoarthritis cartilage. *Arthritis Rheum* 2009; 60: 1035-1041.
- [3] Zilahi E, Tarr T, Papp G, Griger Z, Sipka S and Zeher M. Increased microRNA-146a/b, TRAF6 gene and decreased IRAK1 gene expressions in the peripheral mononuclear cells of patients with Sjogren's syndrome. *Immunol Lett* 2012; 141: 165-168.
- [4] Sonkoly E, Wei T, Janson PC, Saaf A, Lundberg L, Tengvall-Linder M, Norstedt G, Alenius H, Homey B, Scheynius A, Stahle M and Pivarski A. MicroRNAs: novel regulators involved in the pathogenesis of psoriasis? *PLoS One* 2007; 2: e610.
- [5] Xie YF, Shu R, Jiang SY, Liu DL and Zhang XL. Comparison of microRNA profiles of human periodontal diseased and healthy gingival tissues. *Int J Oral Sci* 2011; 3: 125-134.
- [6] Zhu H, Luo H, Li Y, Zhou Y, Jiang Y, Chai J, Xiao X, You Y and Zuo X. MicroRNA-21 in scleroderma fibrosis and its function in TGF-beta-regulated fibrosis-related genes expression. *J Clin Immunol* 2013; 33: 1100-1109.
- [7] Taganov KD, Boldin MP, Chang KJ and Baltimore D. NF-kappaB-dependent induction of microRNA miR-146, an inhibitor targeted to signaling proteins of innate immune responses. *Proc Natl Acad Sci U S A* 2006; 103: 12481-12486.
- [8] Perry MM, Moschos SA, Williams AE, Shepherd NJ, Larner-Svensson HM and Lindsay MA. Rapid changes in microRNA-146a expression negatively regulate the IL-1beta-induced inflammatory response in human lung alveolar epithelial cells. *J Immunol* 2008; 180: 5689-5698.
- [9] Skovgaard K, Cirera S, Vasby D, Podolska A, Breum SO, Durrwald R, Schlegel M and Heegaard PM. Expression of innate immune genes, proteins and microRNAs in lung tissue of pigs infected experimentally with influenza virus (H1N2). *Innate Immun* 2013; 19: 531-544.
- [10] Wang Z, Filgueiras LR, Wang S, Serezani AP, Peters-Golden M, Jancar S and Serezani CH. Leukotriene B4 enhances the generation of

miR-146b upregulated in pulmonary fibrosis

- proinflammatory microRNAs to promote MyD88-dependent macrophage activation. *J Immunol* 2014; 192: 2349-2356.
- [11] Jiang X, Ning Q and Wang J. Angiotensin II induced differentially expressed microRNAs in adult rat cardiac fibroblasts. *J Physiol Sci* 2013; 63: 31-38.
- [12] Kalman S, Garbett KA, Vereczkei A, Shelton RC, Korade Z and Mirnics K. Metabolic stress-induced microRNA and mRNA expression profiles of human fibroblasts. *Exp Cell Res* 2014; 320: 343-353.
- [13] Nal B, Mohr E, Silva MI, Tagett R, Navarro C, Carroll P, Depetris D, Verthuy C, Jordan BR and Ferrier P. Wdr12, a mouse gene encoding a novel WD-Repeat Protein with a notchless-like amino-terminal domain. *Genomics* 2002; 79: 77-86.
- [14] Liao Y, Zhang M and Lonnerdal B. Growth factor TGF-beta induces intestinal epithelial cell (IEC-6) differentiation: miR-146b as a regulatory component in the negative feedback loop. *Genes Nutr* 2013; 8: 69-78.
- [15] Nho RS, Peterson M, Hergert P and Henke CA. FoxO3a (Forkhead Box O3a) deficiency protects Idiopathic Pulmonary Fibrosis (IPF) fibroblasts from type I polymerized collagen matrix-induced apoptosis via caveolin-1 (cav-1) and Fas. *PLoS One* 2013; 8: e61017.
- [16] Liu G, Friggeri A, Yang Y, Milosevic J, Ding Q, Thannickal VJ, Kaminski N and Abraham E. miR-21 mediates fibrogenic activation of pulmonary fibroblasts and lung fibrosis. *J Exp Med* 2010; 207: 1589-1597.
- [17] Yang S, Xie N, Cui H, Banerjee S, Abraham E, Thannickal VJ and Liu G. miR-31 is a negative regulator of fibrogenesis and pulmonary fibrosis. *FASEB J* 2012; 26: 3790-3799.
- [18] Yang S, Cui H, Xie N, Icyuz M, Banerjee S, Antony VB, Abraham E, Thannickal VJ and Liu G. miR-145 regulates myofibroblast differentiation and lung fibrosis. *FASEB J* 2013; 27: 2382-2391.
- [19] Xiao J, Meng XM, Huang XR, Chung AC, Feng YL, Hui DS, Yu CM, Sung JJ and Lan HY. miR-29 inhibits bleomycin-induced pulmonary fibrosis in mice. *Mol Ther* 2012; 20: 1251-1260.